THE ASTROPHYSICAL JOURNAL, 320:454–463, 1987 September 15

THE STRUCTURE AND EVOLUTION OF HOAG'S OBJECT

FRANÇOIS SCHWEIZER[1] AND W. KENT FORD, JR.[1]
Department of Terrestrial Magnetism, Carnegie Institution of Washington
ROBERT JEDRZEJEWSKI
Mount Wilson and Las Campanas Observatories, Carnegie Institution of Washington
AND
RICCARDO GIOVANELLI
Arecibo Observatory, National Astronomy and Ionosphere Center[2]
Received 1987 January 5; accepted 1987 March 3

ABSTRACT

We present new imaging, photometric, and spectroscopic observations of Hoag's object, a 16th magnitude galaxy consisting of an almost perfectly round core surrounded by a faint, apparently detached ring. The core of this distant system ($cz_\odot = 12{,}735$ km s^{-1}) appears to be a normal spheroid for its luminosity ($M_B = -20.43$ for $H_0 = 50$ km s^{-1} Mpc^{-1}), with a well-defined $r^{1/4}$ law, a half-light radius $r_e = 3.6$ kpc, a central velocity dispersion $\sigma_v = 154 \pm 6$ km s^{-1}, and an apparent rotation at $r = 2.5$ kpc of $V_{\rm rot} \sin i = 18$ km s^{-1}. The ring is of comparable luminosity ($M_B = -20.55$), has a mean radius of $18''.5 = 23$ kpc, is inclined about $19° \pm 5°$ to the plane of the sky, and shows knotty structure and gaseous emission lines indicative of young stars. The two-horned 21 cm line profile measured at Arecibo shows that the ring rotates with $V_{\rm max} = 300^{+100}_{-60}$ km s^{-1} and has an H I mass normal for the system's luminosity, $M_{\rm H\,I} = 1.8(\pm 0.2) \times 10^{10}\ M_\odot$. The absolute magnitude of the galaxy is $M_B = -21.24$, and the blue mass-to-light ratio within $r = 32$ kpc is $M/L_B = 14^{+10}_{-5}$ $(M/L_B)_\odot$. Our observations rule out previous hypotheses that the ring may be (1) the gravitationally lensed image of a background galaxy or (2) the ring-wave response of a galactic disk to the central passage of a companion, and provide evidence against the recently advanced hypothesis that (3) the ring formed in response to an extreme bar instability in a galactic disk. Instead, we propose the new hypothesis that Hoag's object owes its structure to a major accretion event at least 2–3 Gyr ago. We point out a number of similar galaxies with presumably equatorial rings that may be fragments resulting from episodic disk formation.

Subject headings: galaxies: evolution — galaxies: individual (Hoag's object) — galaxies: photometry — galaxies: structure — radio sources: 21 cm radiation

I. INTRODUCTION

In 1950, Hoag called attention to a peculiar object in Serpens, which at first sight seemed to be a perfectly symmetrical planetary nebula. On a Jewett Schmidt plate, the object appeared to consist of a diffuse core surrounded by "a perfect halo 17″ in radius." Because of the diffuse core, the lack of emission lines, and the high Galactic latitude ($b = +56°$), Hoag (1950) suggested that alternatively his object might be a pathological galaxy or perhaps even some gravitational lens system.

The extragalactic nature of Hoag's object was established beyond doubt by O'Connell, Scargle, and Sargent (1974), who obtained several spectrograms with the Lick 3 m and Palomar 5 m telescopes and detected in the diffuse core the Ca II H and K absorption lines and the G band at a redshift of $12{,}740 \pm 50$ km s^{-1}. They suggested that the object is a distant compact galaxy surrounded by a large, luminous blue ring. This apparent ring seemed unlikely to be the lensed image of a background galaxy because the intervening gravitational lens would have to possess a mass of over $10^{13}\ M_\odot$ and $M/L_V \approx 1500$ to achieve the required lensing, whereas the absorption lines observed in the core appeared of normal width. Yet the ring spectra were featureless, and the published Crossley plate of the object showed no more structure in the ring than can be seen on the Palomar Sky Survey prints.

On the basis of an improved photograph taken with the Wise 1 m reflector and new photoelectric photometry, Brosch (1985) has recently called Hoag's object a "perfect ringed galaxy" and has suggested that the ring may have been formed a few Gyr ago as the result of an extreme bar instability in a galactic disk. Yet at present the core appears round and unbarred, and Brosch's failure to detect optical emission lines or the 21 cm line of H I from the ring does not permit him to test his hypothesis that this galaxy may lack a massive halo.

The abundance of hypotheses and the paucity of discriminating data, especially for the ring, have been a consequence of the remoteness of Hoag's object. With a recession velocity of 12,822 km s^{-1} relative to the Local Group, this object lies at a nominal distance of 256 Mpc (for $H_0 = 50$ km s^{-1} Mpc^{-1}, adopted throughout this paper). At that distance, an angle of 1″ corresponds to 1.24 kpc; hence, structures smaller than 1 kpc, e.g., individual H II regions or OB associations, cannot be resolved even in excellent seeing. The distance modulus of $(m - M)_0 = 37.04$ mag, too, suggests that only objects or groups of objects brighter than $M_V \approx -12$ stand a chance of being detected on deep CCD frames obtained with large telescopes.

Our curiosity concerning Hoag's object was greatly stimulated after we obtained a first image in 1″ seeing with the 4-Shooter camera of the Hale 5 m telescope at Palomar. When

[1] Guest Investigator at Palomar Observatory.
[2] The National Astronomy and Ionosphere Center is operated by Cornell University under contract with the National Science Foundation.

TABLE 1

LOG OF OBSERVATIONS OF HOAG'S OBJECT

Date (1985)	Telescope (m)	Instrument[a]	Detector	Filter	Integration (s)	Wavelength/Velocity Coverage
May 14.....	5	4C	TI CCD	g	2 × 300	4560–5270 Å
May 21	5	DS	TI CCD	...	5400	5000–5650 Å
June 16	5	4C	TI CCD	i	360	7500–8800 Å
June 16	5	4C	TI CCD	g	240	4560–5270 Å
June 16	5	4C	TI CCD	r	300	6050–6950 Å
July 10	305	21S	GaAS FET	...	7 × 300	11700–13700 km s^{-1}

[a] 4C = 4-Shooter camera, Chip 2; DS = Double spectrograph with 2″ × 120″ slit at P.A. 95°; 21S = 21 cm spectrometer system.

displayed on the TV monitor in the control room of the telescope, this image showed such detailed knotty structure in the ring that the gravitational lens hypothesis for the ring seemed immediately untenable. Yet Hoag's object also looked so unlike any other galaxy, rather resembling a planetary nebula with a diffuse core, that it induced us to make follow-up observations. We present here results based on various CCD images, on an optical spectrogram of the core and ring, and on an H I profile. Section II describes the observations and reduction procedures, § III derives the physical properties of the galaxy and of its components, and § IV discusses various hypotheses for the origin of this interesting system and of related galaxies.

II. OBSERVATIONS

We have observed Hoag's object using three different telescope-instrument combinations: the Hale 5 m telescope at Palomar Observatory with the 4-Shooter camera, the same telescope with the double spectrograph, and the Arecibo 305 m telescope with the 21 cm dual circular feed system. Table 1 gives a log of the individual observations and their wavelength coverage.

a) *gri* Photometry

Our first direct image of Hoag's object was recorded under excellent conditions (seeing = 1.″05 FWHM) with the 4-Shooter camera (Gunn *et al.* 1984) and a Gunn g filter (Thuan and Gunn 1976). A second image in the same passband was obtained immediately following the first, but with the telescope moved 20″ west. The two images, each consisting of 800 × 800 pixels (scale = 0.″334 pixel^{-1}), were later flat-fielded, cleaned of bad columns by interpolation, shifted, and co-added with the image processing system at DTM, which consists of a VAX-11/750 computer plus Gould–DeAnza IP-8500 processor. Figure 1 (Plate 11) shows a 2.′2 × 2.′7 portion of the resulting sum image, representing a total of 10 minutes of exposure. The top four panels of Figure 2 (Plate 12) show a central subsection of the same image at three different contrasts and as an isophotal map.

Further images of Hoag's object in the passbands g, r, and i (Thuan and Gunn 1976; Wade *et al.* 1979) were kindly obtained for us with the same equipment by Drs. R. A. Windhorst and D. C. Koo. Although the sky was covered with cirrus, the data were later calibrated with existing photometry of the galaxy itself, as described below. The bottom two panels of Figure 2 show the processed r and i images. Notice that, apart from the lower signal-to-noise ratio of the r and i images, Hoag's object looks remarkably similar at wavelengths of about 4900 Å (g), 6500 Å (r), and 8100 Å (i).

Table 2 presents photometric data extracted from the *gri* images and corrected for Milky Way absorption corresponding to $E_{B-V} = 0.032$ mag (Burstein and Heiles 1982). Column (1) gives the radius a in arcseconds, column (2) the corrected surface brightness g_0 in units of mag arcsec^{-2}, columns (3) and (4) the color indices $(g - r)_0$ and $(r - i)_0$, and column (5) the apparent ellipticity $\epsilon \equiv (a - b)/a$ of fitted isophotes. The photometric data were extracted with the software package VISTA (Lauer, Stover, and Terndrup 1983). Within the region of the core ($a \lesssim 12''$), brightness and ellipticity profiles were derived by fitting isophotes with concentric ellipses through iterative Fourier analysis (Carter 1978; Kent 1983; Lauer 1985); in this procedure, the variable a corresponds to the semimajor axis of the best-fitting ellipse. The same procedure could not be applied in the region of the ring ($12'' \lesssim a \lesssim 34''$), where the luminosity distribution is too knotty for fitting ellipses. There, we measured the mean surface brightness and

TABLE 2

PHOTOMETRIC DATA[a]

a (1)	g_0 (mag arcsec^{-2}) (2)	$(g - r)_0$ (mag) (3)	$(r - i)_0$ (mag) (4)	ϵ (5)
0.″00.....	18.50	...	...	...
0.33.....	18.61	...	...	...
0.67.....	18.95	...	...	...
1.00.....	19.45	...	...	...
1.34.....	19.92	0.60	0.25	0.041
1.67.....	20.36	0.64	0.24	0.027
2.00.....	20.70	0.64	0.23	0.027
2.67.....	21.28	0.64	0.23	0.027
3.34.....	21.74	0.62	0.23	0.030
4.01.....	22.15	0.60	0.22	0.030
5.01.....	22.69	0.57	0.19	0.028
6.01.....	23.17	0.57	0.19	0.028
7.35.....	23.69	0.54	0.20	0.037
8.68.....	24.15	0.53	0.16	0.043
10.02.....	24.44	0.53	0.06	0.058
11.53.....	24.62	0.51	0.02	...
13.54.....	24.42	0.36	0.25	...
15.54.....	23.93	0.32	0.49	...
18.54.....	23.66	0.27	0.57	...
21.55.....	24.00	0.33	0.52	...
24.55.....	24.59	0.29	0.46	...
27.56.....	25.56	...	...	...
30.57.....	26.41	...	...	...
33.57.....	27.27	...	...	...

[a] Corrected for Milky Way absorptions of $A_g = 0.105$, $A_r = 0.071$, and $A_i = 0.052$ (corresponding to $E_{B-V} = 0.032$).

colors by integrating the flux in concentric circular annuli of mean radius a and dividing the flux by the area.

The surface brightness and colors were calibrated as follows. Since the g image of Figure 1 was obtained under photometric conditions, we determined the zero-point of the g profile from out-of-focus images of a standard star observed shortly before Hoag's object. The estimated error of the zero point is $\lesssim 0.02$ mag. As a check with other observers, we integrated the calibrated g profile within circular apertures and converted the resulting magnitudes to the V passband. Our converted V-magnitudes agree with V-magnitudes measured by Brosch (1985) in 15″ and 58″ apertures to within $+0.10$ mag and -0.17 mag, respectively, and agree with unpublished photoelectric scanner measurements made by Dr. R. W. O'Connell through a 9″ aperture (see O'Connell, Scargle, and Sargent 1974) to within 0.1 mag.

Since our r and i images were obtained through cirrus, we calibrated the color indices $g - r$ and $r - i$ with the above-mentioned scanner fluxes measured by Dr. O'Connell. The internal scatter of our color indices is typically 0.03 mag, whereas the calibrating scanner measurements have a quoted mean error of 0.07 mag. Therefore, the mean errors of the $(g - r)_0$ and $(r - i)_0$ indices given in Table 2 are estimated to be $\lesssim 0.10$ mag.

The integrated magnitude of Hoag's object within the $g_0 = 25$ mag arcsec^{-2} isophote (radius = 25″.6) is $g_0 = 15.26$ mag after correction for Milky Way absorption, which corresponds to $V_0 \approx g_0 - 0.35(g - r)_0 = 15.1$. The asymptotic total magnitude is ~ 0.1 mag brighter and does not increase measurably beyond $r = 45''$.

b) *Optical Spectroscopy*

To measure radial velocities in the core and ring, we obtained a long-slit spectrogram of Hoag's object with the red camera of the double spectrograph (Oke and Gunn 1982) on the Hale 5 m telescope. The 1200 line mm^{-1} grating, combined with the Texas Instruments CCD detector (15 μm pixels) and a 2″ slit, yielded a reciprocal dispersion of 0.8 Å pixel^{-1} and a resolution of 2.8 Å (FWHM). The scale and resolution perpendicular to the dispersion were 0″.49 pixel^{-1} and 1″.6, respectively. The 2″ × 120″ slit was placed across the nucleus at a position angle of 95°, roughly aligned with the apparent major axis of the ring and intersecting a relatively bright knot in the eastern part. The exposure time was 5400 s.

The CCD frame was reduced using methods similar to those of Tonry (1984). After bias subtraction and division by the spectrum of an incandescent lamp, bad pixels due to cosmic rays were removed mostly automatically and, in some cases, also by hand. Wavelength calibration and geometrical rectification were accomplished by fitting polynomials to 45–50 lines of a separate comparison spectrum and to images of seven holes spaced evenly along the slit and illuminated by an incandescent lamp. Wavelength residuals were 0.14 Å (rms) after a single cycle of 2 σ rejection, and position residuals were 0″.08 rms. The polynomial coefficients $\lambda(x, y)$ and $z(x, y)$ were then used to rebin the spectrogram of Hoag's object onto a grid spaced evenly in log λ (1024 increments from $\lambda\lambda$5000–5645) and in position along the slit (200 increments of 0″.5 each). A night-sky spectrum was extracted from two strips near the ends of the slit ($\sim 50''$ from the center of Hoag's object) and subtracted from the whole frame. Major night-sky lines that subtracted imperfectly were interpolated over.

To obtain velocities and velocity dispersions at different positions along the slit, the processed spectrogram was subdivided into strips of varying width. Rows in each strip were co-added so that the total number of counts in the resulting spectrum exceeded 2×10^5. For the Fourier-quotient analysis, spectra were also extracted from CCD frames of five K giant standards observed on the same night, and a composite template spectrum was formed by rebinning the spectra to the same velocity and co-adding them. Finally, the absolute velocity of the template spectrum was found by cross-correlating the latter with a spectrum of the night sky.

Figure 3 shows the resulting spectra of the five combined K giants, the core of Hoag's object, and a 2″ × 6″ segment of the ring located 17″ east of the nucleus. The spectrum of the core is characteristic of an old stellar population, featuring prominently the Mg I triplet and various blended Fe I lines, and weakly, if at all, Hβ in absorption; no emission lines are seen. The spectrum of the ring shows, superposed on a weak continuum, two emission lines indicative of ionized gas: Hβ and [O III] λ5007. These lines are visible only on the eastern side of the ring.

Figure 4 shows velocities and velocity dispersions in the core as functions of position along the slit. They were measured from individual rows of the two-dimensional core spectrum by the Fourier-quotient technique (Simkin 1974; Sargent *et al.* 1977). The systemic velocity derived from eight data points within $|r| \leq 2''$ is $cz_\odot = 12{,}735 \pm 4$ km s^{-1} (heliocentric). The mean velocity dispersion in the same interval is $\sigma_v = 154 \pm 6$ km s^{-1}.

c) *21 Centimeter Line Observations*

In order to search for H I emission, we observed Hoag's object with the Arecibo 305 m telescope for a total of about 100 minutes (see Table 1). The observing sequence consisted of seven 300 s integrations on the source interleaved with seven integrations of the same duration off the source. We used the dual circular feed, tuned to 1370 MHz, with the 1008 channel autocorrelation spectrometer in a 4 × 252 channel mode, each quadrant covering a 10 MHz band around $cz_\odot = 12{,}700$ km s^{-1}. Two circularly polarized components of the signal were collected separately and fed each to two spectrometer quadrants. The channel separation was 8.6 km s^{-1}.

Figure 5 displays the final 21 cm line profile, which shows the two-horned shape typical of rotating disk galaxies. The profile has been smoothed to an effective resolution of 15 km s^{-1}, and its low-velocity side has been corrected as well as possible for effects of a severe narrow-band interference. This interference of unknown origin introduced some ringing, but could be largely suppressed by removing the most affected channel and by subsequent smoothing. The main effects remaining are (1) an uncertain slope on the low-velocity side of the profile and (2) a spurious spike near $v = 13{,}200$ km s^{-1}.

The integrated flux in the 21 cm line is 1.04 Jy km s^{-1}. After correction for random pointing errors and beam dilution (Haynes and Giovanelli 1984), the value becomes 1.15 ± 0.10 Jy km s^{-1}. The heliocentric systemic velocity is $cz_\odot = 12{,}736 \pm 6$ km s^{-1}. The profile width measured at 50% of the average intensity is 239 ± 10 km s^{-1}, while at 50% of the peak intensity the value is 204 ± 10 km s^{-1}. The latter value is discussed further in § III*c*.

III. RESULTS

This section describes the physical properties of the galaxy and of its components.

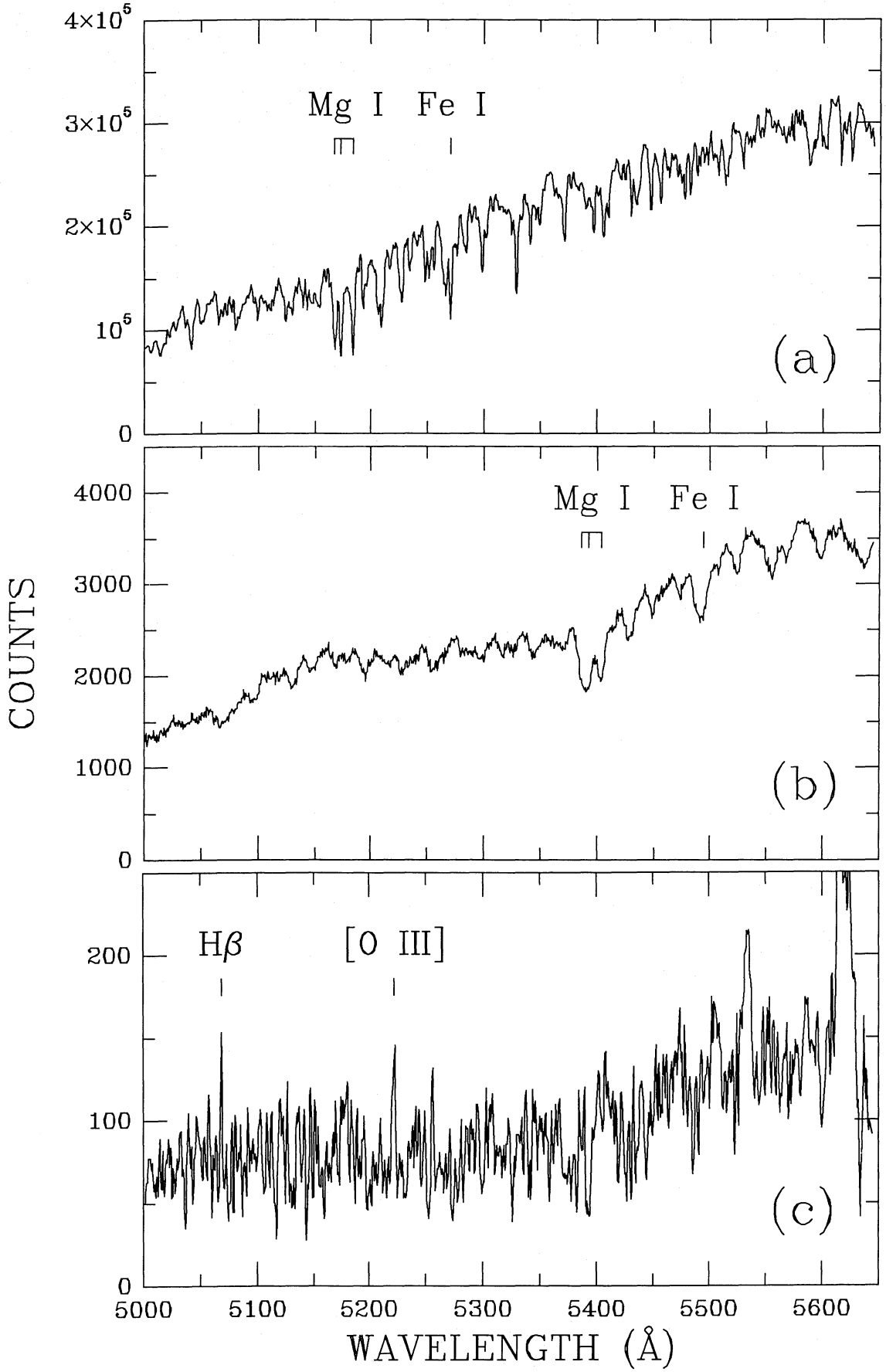

FIG. 3.—Spectra of (*a*) five K giants combined, (*b*) the core of Hoag's object, and (*c*) the ring. The core spectrum refers to a central region of 2″ × 4″, whereas the ring spectrum refers to a 2″ × 6″ box oriented at P.A. = 95° and centered on the ring at 17″ east of the nucleus. The ring spectrum has been smoothed slightly to diminish noise. These spectra were obtained with the double spectrograph of the Hale 5 m telescope. Note the old population characteristics of the core spectrum and the weak Hβ and [O III] λ5007 emission lines of the ring.

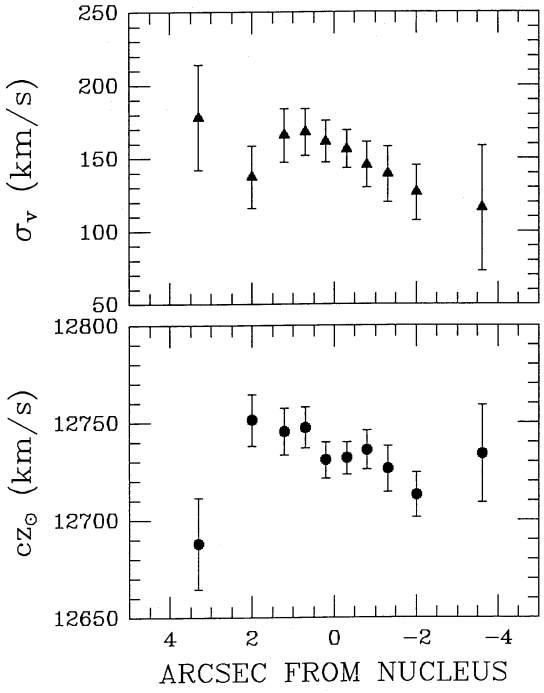

FIG. 4.—Heliocentric radial velocities (*bottom*) and velocity dispersions (*top*) measured in the core of Hoag's object as a function of position along the slit (oriented at P.A. = 95°). The apparent rotation of the core is slow out to $r = 2'' = 2.5$ kpc and ill determined beyond.

a) Velocities and Physical Association

The systemic velocities measured for the core and ring agree well. The velocity of the core determined from absorption lines is $cz_\odot = 12{,}735 \pm 4$ km s^{-1}, whereas that of the ring determined from the H I profile is $cz_\odot = 12{,}736 \pm 6$ km s^{-1}. Therefore, the physical association of core and ring is established beyond doubt, and a gravitational lens, already unlikely from the image of the ring, is ruled out.

One could conceivably argue that the H I profile may originate in the core rather than in the ring. Yet velocities measured from the weak Hβ and [O III] λ5007 lines in the eastern part of the ring agree roughly with those in the H I profile, thus confirming that the ring has the same velocity as the core. Specifically, measurements of Hβ in five eastern locations yield a mean velocity of 12,788 $\pm$ 9 km s^{-1} (at $\langle r \rangle \approx 20''$), and measurements of the very noisy [O III] λ5007 profile in two locations yield 12,876 $\pm$ 50 km s^{-1} (estimated error). Although the agreement between the two lines is poor, both velocities agree roughly with the high-velocity horn of the H I profile (Fig. 5), suggesting that, relative to the core, the east side of the ring is rotating away from us.

b) Brightness Profile and Components

Figure 6 displays the profile of mean surface brightness g_0 in Hoag's object as a function (*a*) of linear radius and (*b*) of $r^{1/4}$. Both forms of the profile show immediately that the apparent gap between the core and the ring contains luminous matter, as found already by Brosch (1985), and as can also be seen directly in Figure 2. At its faintest, the material in the gap has a mean surface brightness of $g_0 = 24.61$ mag arcsec^{-2} and is 0.96 mag fainter than the peak of the azimuthally averaged ring.

Figure 6*b* also shows very clearly that *the core is a normal spheroid.* Over at least 5 mag in surface brightness, it is described remarkably well by an $r^{1/4}$ law (de Vaucouleurs 1953; Kormendy 1977).[3] The half-light radius of this spheroid (extended as shown by the dashed line in Fig. 6*b*) is $r_e = 2''.9 = 3.6$ kpc. The surface brightness at that radius is $g_0(r_e) = 21.48$ mag arcsec^{-2}, which, after a *K*-correction and a correction for *z*-dimming, transforms to $B_e = 21.97$ mag arcsec^{-2}. This value is only 0.68 mag fainter than the mean value $B_e = 21.29$ mag arcsec^{-2} expected for ellipticals of the same r_e, and lies well within the range observed for bulges of disk galaxies (Kormendy 1980, eq.[3] and Fig. 8).

The apparent core radius of the spheroid, defined as the radius at which the apparent surface brightness reaches half the central value, is $r_{c,\mathrm{app}} = 0''.90$. This radius, when combined with the measured point-spread function and tabulations of seeing effects (Schweizer 1981), indicates that the core of the spheroid is virtually unresolved: the nominal ratio between the

[3] Brosch's (1985) conclusion that the core may be fitted as well by an exponential disk as by an $r^{1/4}$ law is mistaken. This conclusion is based on a plot of the logarithm of surface brightness against the logarithm of radius, in which the core is fitted reasonably well by a straight line (Brosch's Fig. 4). However, such a line in double-logarithmic coordinates represents a power law rather than an exponential. It has long been known, of course, that the light distribution of spheroids and ellipticals can be approximated roughly by a power law of the form $\log (i/i_0) = -2 \log (r/a + 1)$, where *i* is the intensity and *a* is a scale parameter (Hubble 1930; also Reynolds 1913).

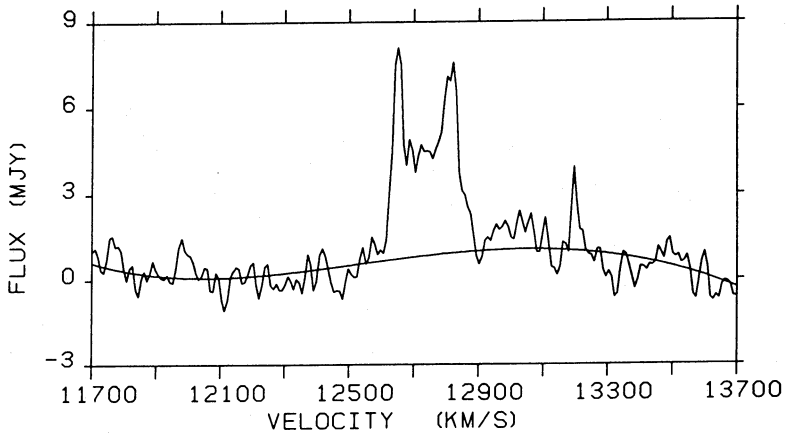

FIG. 5.—Twenty-one centimeter line spectrum of Hoag's object obtained with the Arecibo 21 cm dual circular feed system. The velocity is heliocentric $cz_\odot$. Superposed on the spectrum is the polynomial baseline which has been subtracted for measuring the flux, systemic velocity, and profile width.

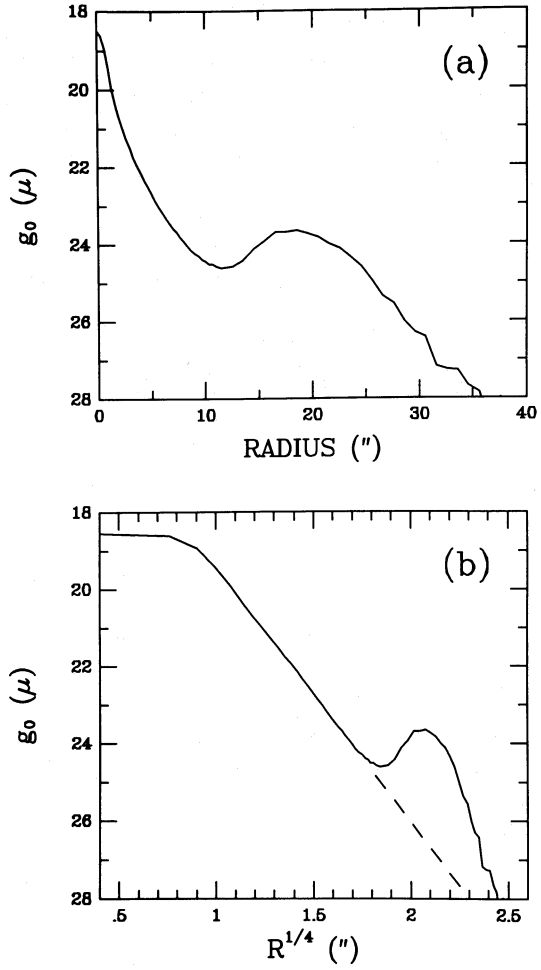

FIG. 6.—Azimuthally averaged surface brightness g_0 in Hoag's object plotted (*a*) as a function of linear radius and (*b*) as a function of $r^{1/4}$. Note the gap of nearly 1 mag depth between core and ring. The core is well represented by an $r^{1/4}$ law and seems to be a normal spheroid. The dashed line represents the extrapolated spheroid used to estimate the integrated magnitudes of spheroid and ring and the bulge-to-disk ratio.

true and apparent core radius is $r_c/r_{c,\mathrm{app}} = 0.25$. Assuming that this ratio is rather an upper limit, the true core radius would be $r_c \lesssim 0''.22 = 280$ pc. This upper limit is certainly consistent with the mean $\langle r_c \rangle = 100$ pc found by Kormendy (1985) for the resolved cores of spheroids and ellipticals of the same absolute magnitude ($M_B = -20.4$) as the spheroid of Hoag's object. Therefore, this spheroid seems to be normal in every photometric respect. Also, it must either be seen close to pole-on or it must be nearly spherical, since it appears almost perfectly round. Its apparent ellipticity as a function of radius varies in the range $\epsilon \equiv (a-b)/a = 0.027$–$0.058$ with a mean value $\langle \epsilon \rangle \approx 0.03$ (Table 2, col. [5]). The major axis points approximately to P.A. = 19° ± 5°.

The *ring* appears as a hump in the profile of surface brightness (Fig. 6). The azimuthally averaged surface brightness reaches a maximum at $r = 18''.5 = 23$ kpc of $g_0 = 23.66$ mag arcsec^{-2} ($V_0 \approx 23.6$ mag arcsec^{-2}, $B_0 \approx 24.2$ mag arcsec^{-2}), explaining why the ring appears so faint on the Palomar Sky Survey prints and in the Crossley photograph shown by O'Connell, Scargle, and Sargent (1974). At a surface brightness of $g_0 = 24.5$ mag arcsec^{-2}, the ring's inner edge lies at $r = 13'' = 16$ kpc and its outer edge at $r = 24'' = 30$ kpc; hence the ring covers a factor of about 2 in radius. Figure 6*a* suggests that beyond $r \approx 23''$, the surface brightness falls off exponentially. Various fits of straight lines yield a slope of ~ 0.30 mag arcsec^{-1}, an exponential scale $\alpha = 3''.7 = 4.6$ kpc, and an extrapolated central surface brightness $g_0(r=0) \approx 17.5 \pm 0.5$ mag arcsec^{-2}. Since the fit is restricted to $r = 23''$–$36''$, it covers only about 3.5 scale lengths. This limited range, the exceptionally high value of $g_0(r=0)$, and the nonexponential inner region suggest that the ring is unusual and ought not to be regarded as merely an exponential disk with a central hole.

Like the spheroid, the ring appears nearly round. To estimate its shape despite its knotty brightness distribution, we smoothed the *g* image with a Gaussian of 2".0 FWHM, plotted isophotes of the smoothed image as shown in Figure 2, and drew smooth curves through the still noisy isophotes. The resulting curves at $g_0 = 25$ and 26 mag arcsec^{-2} can be represented roughly by ellipses with ellipticity $\epsilon = 0.07 \pm 0.02$ and 0.05 ± 0.02 and major axes at P.A. = 75° ± 10° and 91° ± 10°, respectively. If interpreted as projections of an inclined, exactly circular structure, these ellipses would suggest an inclination of the ring to the plane of the sky somewhere in the range $i = 14°$–$24°$ (where $i = 0°$ is face-on).

Visual magnitudes for each component can be derived by integrating the brightness profile and transforming g_0 to V_0 through the approximate relation

$$V_0 \approx g_0 - 0.35(g-r)_0 \, . \qquad (1)$$

After applying a *K*-correction of 0.11 mag, and denoting *K*-corrected quantities by the subscript $z = 0$, we find $V_{0,z=0} = 15.72$ for the core within $r = 12''$ and $V_{0,z=0} = 15.80$ for the ring between $r = 12''$ and $26''$ (the outer radius corresponding to the $V_0 = 25$ mag arcsec^{-2} isophote). However, Figure 6*b* suggests that it may be more appropriate to decompose the light into a spheroid extending under the ring (*dashed line*) and a ring consisting of the excess light. In this case, and again within the boundary of the $V_0 = 25$ mag arcsec^{-2} isophote, the magnitudes of spheroid and ring are $V_{0,z=0} = 15.65$ and 15.94, respectively, yielding a visual bulge-to-"disk" ratio $(\mathscr{B}/\mathscr{D})_V = 1.31$. In the Johnson passband *B*, the corresponding values are $B_{0,z=0}$(spheroid) = 16.61, $B_{0,z=0}$(ring) = 16.49, and $(\mathscr{B}/\mathscr{D})_B = 0.90$. The *B*-magnitudes were obtained from the *V*-magnitudes by adding $(B-V)_{0,z=0} = 0.96$ for the spheroid and 0.55 for the ring; these color indices are based on photoelectric measurements by Brosch (1985) and have been corrected for Milky Way extinction and a *K*-term due to the redshift (Pence 1976). The absolute blue magnitude of the spheroid is then $M_B = -20.43$, that of the ring is -20.55, and that of the whole system is -21.24.

c) *Kinematics*

The spheroid has a central velocity dispersion of $\sigma_v = 154 \pm 6$ km s^{-1} (§ II*b*) and a blue absolute magnitude $M_B = -20.43$ (§ III*b*). From the mean relation $M_B = +1.26 - 9.76 \log \sigma_v$ for 19 bulges of spiral galaxies (Whitmore and Kirshner 1981), one would expect $M_B = -20.09$ for the measured σ_v, with an rms residual of 0.9 mag. Therefore, the spheroid of Hoag's object has a normal velocity dispersion for its luminosity.

The spheroid seems to rotate in the same direction as the ring, with the east side receding (Fig. 4), if we ignore the outermost measurements with large error bars at 3".3 east and 3".6 west of the nucleus. The apparent rotation is then $V_{\mathrm{rot}} \sin i \approx$

18 km s^{-1} at $r = 2''.0 = 2.5$ kpc, yielding $V_{rot} \approx 37$–55 km s^{-1} if we assume that the spheroid has the same inclination as the ring, $i = 29°$–$19°$ (§ III*b*). Although the data for comparison are sparse, this velocity range agrees roughly with velocities measured at the same radius in galaxies with comparable bulge luminosities (Kormendy and Illingworth 1982). Therefore, the spheroid of Hoag's object appears to be normal not only in its photometric properties but also in its kinematic properties.

The rotational velocity of the ring is difficult to determine because of the ring's nearly face-on orientation. Given the rather uncertain emission-line velocities measured on the east side of the ring and the lack of detected optical emission on the west side, we must rely on the H I profile (Fig. 5) to determine the rotational velocity. Model calculations suggest that in high-luminosity galaxies with two-horned profiles the profile width at 50% of the peak, W_{50}, is a good measure of twice the maximum rotational velocity V_{max} (Thonnard *et al.* 1980), and that corrections for internal velocity dispersion are also minimal there (Bottinelli *et al.* 1983). Hence, we take

$$V_{max} = \frac{W_{50}}{2 \sin i \, (1 + z)}, \qquad (2)$$

which with $W_{50} = 204$ km s^{-1} yields $V_{max} = 97.8/\sin i$ km s^{-1} $= 300^{+100}_{-60}$ km s^{-1} for $i = 19° \pm 5°$. For comparison, an average Sa galaxy of the same luminosity as Hoag's object ($M_B = -21.24$) rotates with $V_{rot} \approx 226$ km s^{-1} at $r = 0.8R_{25}$, where R_{25} is the radius of the $B = 25$ mag arcsec^{-2} isophote (Rubin *et al.* 1985). Therefore, within the uncertainties the rotation of the ring, too, seems to be normal for the luminosity of the object. Note that the classical two-horned shape of the H I profile implies a rather flat rotation curve, as one would expect for a galaxy of relatively high luminosity (Thonnard *et al.* 1980).

d) Gas Content

The mass of neutral hydrogen derived from the integrated and corrected 21 cm line flux F_{21} (§ II*c*) is $M_{HI} = 2.36 \times 10^5 D^2 F_{21} = 1.8(\pm 0.2) \times 10^{10} M_\odot$ (for D in Mpc and $H_0 = 50$). This mass is nearly 4 times higher than the upper limit determined by Brosch (1985) from a nondetection with the Westerbork Synthesis Radio Telescope. Yet the profile shown in Figure 5 leaves no doubt that emission from the galaxy has been detected and suggests that the measuring error is $\lesssim 20\%$. Further support for our value of M_{HI} comes from the fact that the H I surface density, when averaged over the linear optical diameter, is normal. This surface density has been shown to be nearly constant for disk galaxies of all Hubble types (Haynes and Giovanelli 1984, esp. Fig. 7). Therefore, even in its gas content Hoag's object appears normal.

In trying to estimate the recent history of the material in the ring, the amount of ionized gas and the star formation rate are of interest. We have measured equivalent widths of Hβ at five positions covered by the spectrograph slit between 16″ and 26″ east. The mean equivalent width is $\langle$EW(Hβ)$\rangle = 1.8$ Å, with an estimated uncertainty of about a factor of 2. On the west side, our failure to detect Hβ implies EW(Hβ) $\lesssim 1.0$ Å. Since many measurements of equivalent widths of Hα, but not of Hβ, have recently become available for various types of galaxies, we must convert EW(Hβ) to EW(Hα) for a comparison. Without absorption and for intermediate to old populations, the ratio is EW$_0$(Hα)/EW$_0$(Hβ) ≈ 3 because of the Balmer decrement and the near-constancy of the continuum flux F_λ. With the mean absorption $A_{H\alpha} = 1.1 \pm 0.5$ mag found by Kennicut and Kent (1983), the ratio becomes EW(Hα)/EW(Hβ) ≈ 5. Therefore, our observations at Hβ suggest that $0 \leq$ EW(Hα) $\lesssim 10$ Å and that star-forming activity in the ring of Hoag's object is as low as in the disk of an Sa or Sab galaxy.

Finally, Table 3 summarizes our results for Hoag's object.

IV. DISCUSSION

Despite our improved knowledge of the structure and dynamics of Hoag's object we have found no reliable clues concerning its origin. It is definitely easier to say what Hoag's object is not than what it is and how it came to be. Therefore, we first review various old hypotheses about its structure and origin. Then we try to redefine in which sense Hoag's object is abnormal and to estimate how frequent similar objects are. Finally, we put forward the new hypothesis that Hoag's object owes it structure to an accretion event some time ago.

a) Review of Old Hypotheses

The most intriguing hypothesis, made by Hoag (1950) in his discovery announcement, is that the ring of the object may be the gravitationally lensed image of a background galaxy. Yet Hoag himself and O'Connell, Scargle, and Sargent (1974) have emphasized that the central core would have to be extraordinarily massive for its luminosity to form the ring by lensing. Our observations rule out this hypothesis in a more direct manner: the ring has the same redshift as the central, supposedly lensing object. Therefore, the ring must be physically associated with the central spheroid and cannot be the lensed image of a background galaxy.

The possibility that Hoag's object may be a classical ring galaxy seen face-on can also be ruled out. In such galaxies, a compact companion has recently punched through a disk galaxy and has set up a ring-shaped density wave (Lynds and Toomre 1976; Theys and Spiegel 1977). For this mechanism to work, the relative velocity of the two galaxies has to be of the order of 10^2 km s^{-2}. Yet the velocity difference between the core and ring of Hoag's object is only -1 ± 7 km s^{-1} (§§ II*b* and II*c*). Since there is no nearby companion galaxy that could have acted as a bullet (Fig. 1), the core is the sole candidate for this purpose, yet it lies at rest relative to the ring. Therefore, Hoag's object cannot be a classical ring galaxy seen with its companion superposed, and its core and ring must form one single object.

O'Connell, Scargle, and Sargent (1974) and Brosch (1985) have argued that (1) the ring cannot consist of light scattered from the core and (2) the gap between core and ring is unlikely to be caused by dust obscuration. Our high-resolution image, the detection of emission lines in the ring but not in the core, the color indices in the gap (Table 2), and the undisturbed $r^{1/4}$ law of the spheroid right into the gap region (Fig. 6) all strongly support these two conclusions.

Brosch (1985) has recently put forth the hypothesis that the ring of Hoag's object may have formed in response to a strong bar instability in a disk a few Gyr ago. According to Brosch, the bar itself has now dissolved, but the galaxy should still be marked by the lack of a heavy halo. Our admittedly rather uncertain value for the rotational velocity, $V_{max} = 300^{+100}_{-60}$ km s^{-1} (§ III*c*), does not confirm this prediction. The integrated mass (in $M_\odot$) within radius R (in kpc) is

$$M(R) = 2.3265 \times 10^5 R V^2, \qquad (3)$$

TABLE 3

PARAMETERS OF HOAG'S OBJECT

Parameter	Symbol	Value
Right ascension	$\alpha(1950)$	$15^h15^m01^s$
Declination	$\delta(1950)$	$+21°46'00''$
Galactic longitude	l	31°.52
Galactic latitude	b	+56°.45
Heliocentric velocity	$cz_\odot$	$12{,}735 \pm 4$ km s^{-1}
Velocity relative to Local Group	cz_{LG}	12,822 km s^{-1}
Distance ($H_0 = 50$)	Δ	256 Mpc
Distance modulus ($H_0 = 50$)	$(m - M)_0$	37.04
Apparent blue magnitude[a]	$B_{0,z=0}$	15.80 ± 0.05
Absolute blue magnitude	M_B	-21.24
Mass within $r = 32$ kpc	M_r	$7^{+5}_{-3} \times 10^{11}\ M_\odot$
M/L_B within $r = 32$ kpc	M/L_B	$14^{+10}_{-5}\ (M/L_B)_\odot$
Spheroidal component ("core"):		
Apparent radius at $g_0 = 24.5$ mag arcsec^{-2}	$R_{24.5}$	10".3 = 12.8 kpc
Mean ellipticity	ϵ	0.034 ± 0.003
Major-axis position angle	P.A.	$19° \pm 5°$
Half-light radius	r_e	2".9 = 3.6 kpc
Blue surface brightness at r_e	B_e	21.97 mag arcsec^{-2}
Apparent blue magnitude[a]	$B_{0,z=0}$	16.61
Absolute blue magnitude	M_B	-20.43
Color index[b]	$(B-V)_{0,z=0}$	+0.96
Blue bulge-to-ring ratio	$(\mathscr{B}/\mathscr{D})_B$	0.90
Central velocity dispersion	σ_v	154 ± 6 km s^{-1}
Measured rotation at $r = 2.5$ kpc	$V_{rot} \sin i$	18 km s^{-1}
Ring component:		
Inner radius at $g_0 = 24.5$ mag arcsec^{-2}	$r_{24.5}$	13".0 = 16.1 kpc
Outer radius at $g_0 = 24.5$ mag arcsec^{-2}	$R_{24.5}$	24".2 = 30.1 kpc
Outer radius at $g_0 = 27$ mag arcsec^{-2}	R_{27}	31".3 = 39.0 kpc
Mean ellipticity	ϵ	0.06 ± 0.02
Major-axis position angle	P.A.	$83° \pm 10°$
Inclination to plane of sky	i	$19° \pm 5°$
Maximum surface brightness at $r = 23$ kpc	B_0	24.2 mag arcsec^{-2}
Apparent blue magnitude[a]	$B_{0,z=0}$	16.49
Absolute blue magnitude	M_B	-20.55
Color index[b]	$(B-V)_{0,z=0}$	+0.55
Integrated 21 cm line flux	F_{21}	1.15 ± 0.10 Jy km s^{-1}
Total H I mass	M_{HI}	$1.8(\pm 0.2) \times 10^{10}\ M_\odot$
Maximum rotation velocity	V_{max}	300^{+100}_{-60} km s^{-1}

[a] Corrected for Milky Way absorption and energy shift (K-term; see text).
[b] From Brosch 1985, corrected for Milky Way reddening and energy shift.

where circular orbits and a spherical potential are assumed. Since the two-horned H I profile is typical of galaxies with flat or slightly rising rotation curves (Thonnard *et al.* 1980), we assume $V(R) = V_{max}$ at $R_{25} = 26'' = 32$ kpc, whence $M(R_{25}) = 6.8 \times 10^{11}\ M_\odot$ with a factor of ~ 1.7 uncertainty. With $M_B = -21.24$, the mass-to-light ratio is $M/L_B = 14^{+10}_{-5}$ and is, therefore, *high* rather than low when compared with $M/L_B = 6$, 4, and 2 for Sa, Sb, and Sc galaxies, respectively (Rubin *et al.* 1985). Because most of the error in M/L_B stems from the uncertain inclination of the ring to the plane of the sky, we guess that the true M/L_B is near or below the lower limit of the indicated range, and the ring inclination is near or above the upper limit $i = 24°$ derived earlier. However, in order for M/L_B to be small, say $M/L_B \lesssim 3$, the inclination would have to be $i \gtrsim 47°$, and the ring would have to be intrinsically elliptical and projected to a near-circle by chance. This geometry appears contrived, and there seems to be no evidence for an abnormally weak halo.

A strong bar instability in the recent past seems also unlikely because the core of Hoag's object is a spheroid and not a disk (§ III*b*, esp. footnote 3). Yet a disk is needed to give rise to a bar instability. Of course, we cannot rule out the possibility that the core was a more elongated triaxial body in the past than it is now, in which case its effect on outlying gas would then perhaps have been similar to that envisaged by Brosch (1985). But we see no cogent reason for assuming this kind of situation, nor is there a well-established mechanism that would make a triaxial galaxy evolve into a rotationally symmetrical body.

b) Normality versus Abnormality

Our observations suggest that Hoag's object is a normal galaxy in most respects. The core seems to be a normal spheroid in all its photometric and kinematic properties. It is neither unusually compact, as O'Connell, Scargle, and Sargent (1974) judged probably because of the large distance, nor a dwarf elliptical, as Brosch (1985) concluded because of his mistaken interpretation of the brightness profile. To the extent that the core resembles an elliptical, its absolute magnitude $M_B = -20.43$ places it among the giant ellipticals of intermediate luminosity. Our optical rotation measurements (Fig. 4) seem to favor a normal bulge in rotation, but better data are needed to adjudicate decisively between a bulge and an elliptical. The ring is definitely flat, as O'Connell *et al.* guessed and as Brosch concluded from the brightness profile. In light of the two-

horned H I profile, a thick shell instead of a ring can now be excluded for certain.

The one major abnormality is the prominent gap in the light distribution between spheroid and ring. From Figure 6*b* we conclude that there is no trace of a disk within $r^{1/4} \leq 1.7$ or $r \leq 8'' = 10$ kpc. Brightness profiles with an apparent deficiency of light in the transition zone between spheroid and exponential disk are known to occur in a small fraction of nearby spirals and have been called "type II" by Freeman (1970). Therefore, one may choose to describe Hoag's object as a galaxy with an extreme type II profile, although this does not clarify the origin of the gap. As the following subsection discusses, there exist galaxies with similarly detached and bright rings, but their central bodies appear nearly always elongated and are probably mostly barred. Therefore, a complete description of the abnormality of Hoag's object may be that it has a detached ring instead of a disk, yet is virtually unbarred.

c) Frequency of Hoag-Type Galaxies

In the following, we loosely group together galaxies with (1) central bodies that are neither obviously barred nor obviously inclined disks and (2) detached outer rings that contain a significant fraction of the total luminosity ($\gtrsim 20\%$), and call them Hoag-type galaxies.

A comparison of Figure 1 with various compilations of galaxy photographs shows that Hoag-type galaxies are rare. We know of no high-resolution photograph of any galaxy that resembles the bull's-eye view of Hoag's object closely. If viewed at higher inclination, the ring of Hoag's object would, of course, appear more elliptical, and the spheroid might appear more elongated depending on the degree of its oblateness. O'Connell, Scargle, and Sargent (1974) mention four relatively bright galaxies that it might then resemble: NGC 2859, NGC 3081, NGC 6028, and IC 5285. Yet we find that at least three of them differ in some distinct way from Hoag's object. NGC 2859 is described by Sandage (1961, p. 42) as a type example of the $SB0_2$ class with a fuzzy and indistinct bar; NGC 3081 shows an elongated core and two spiral arms which nearly overlap each other (Sandage 1961. p. 11); and IC 5285 has either an inner disk or a strong bar. Clearly, neither of these descriptions fits Hoag's object. Only NGC 6028 resemble's Hoag's object, at least at the resolution available on the prints of the Palomar Observatory Sky Survey. It is shown in Figure 7*b* (Plate 13).

To search for Hoag-type galaxies in a larger volume of space and to determine their relative frequency, one has to resort to the Palomar Observatory or ESO/SRC sky surveys. Because of their lower spatial resolution, these surveys yield lists of candidate objects with a wider dispersion of characteristics. Fine samples of ringed galaxies selected in this manner have been presented by Vorontsov-Vel'yaminov (1960) and Buta (1986). We ourselves have looked at two different samples.

One unpublished sample was selected years ago by Dr. Morton S. Roberts, who searched the glass copies of the Palomar Observatory Sky Survey (POSS) for galaxies with faint outer rings and kindly put his surviving coordinate list and notes at our disposition. We have inspected all 69 objects of his list on POSS prints and find nine that resemble Hoag's object to some degree. One of these nine is Hoag's object itself, which Dr. Roberts's notes describe as "star with perfect ring." Of the remaining eight, one has a strongly barred central component and four have weakly barred ones. Therefore, by our definition there are only four Hoag-type galaxies left in this sample, one of which is Hoag's object itself. Panels *a*, *c*, *d*, and *e* of Figure 7 show these four galaxies, all reproduced from the blue POSS prints.

Our second sample stems from a careful survey of 11 fields of the southern SRC(J) sky survey at high Galactic latitude. In searching the film copies of these fields for polar-ring galaxies some years ago (Schweizer, Whitmore, and Rubin 1983), we noted six Hoag-type galaxies. For three of these, we determined redshifts with the Reticon spectrograph of the du Pont 2.5 m telescope at Cerro Las Campanas, Chile. Table 4 gives the coordinates, heliocentric velocities, outer-ring diameters, estimated apparent magnitudes, and absolute magnitudes of these three galaxies and of the other five specimens shown in Figure 7. From the estimated mean apparent magnitude of the six Hoag-type galaxies, $\langle m_B \rangle = 16.7$, and the number of galaxies (Rainey 1977) brighter than the magnitude set by the faintest object, $m_B \approx 17.5$, we estimate that the fraction of galaxies that look like Hoag's object at $\sim 2''$ resolution is roughly 4×10^{-4}. Assuming that only about half of all possible candidate galaxies are viewed sufficiently close to face-on to be recognized as being of Hoag's type, the true fraction of Hoag-type galaxies is probably close to 1×10^{-3}.

In summary, galaxies with detached rings comparable in brightness and diameter to the ring of Hoag's object do exist in small numbers, as recognized already by Vorontsov-Vel'yaminov (1960). The majority of these galaxies seem to be barred, and only a minority fall into the class of Hoag-type

TABLE 4

HOAG-TYPE GALAXIES SHOWN IN FIGURE 7

NAME	α(1950)	δ(1950)	$cz_\odot$	SOURCE	RING[a] D''	RING[a] D_{kpc}	m_B	SOURCE	A_B	M_B	FIGURE 7 PANEL
A0036.4−3905	$00^h36^m22^s$	−39°05′.5	30090	1	28	82	17.0	4	0.00	−21.9	*f*
A0247.9−4015	02 47 52	−40 15.0	19480	1	27	51	16.5	4	0.00	−21.4	*g*
A0452.3−4256	04 52 16	−42 56.6	24896	1	25	60	17.0	4	0.00	−21.5	*h*
MCG−2-33-25	12 48 17	−09 35.3	...		50	...	15.5	4	0.04	...	*c*
Hoag's object	15 15 01	+21 46.0	12735	2	48	60	16.1	2	0.13	−21.1	*a*
A1519.6+5451	15 19 35	+54 51.2	...		37	...	16.5	4	0.00	...	*d*
NGC 6028	15 59 12	+19 29	4480	3	65	29	14.0	5	0.10	−20.9	*b*
Zw 167.025	16 04 38	+27 59.3	...		34	...	15.4	6	0.11	...	*e*

[a] Ring diameters measured from sky survey prints or films; linear diameters are for $H_0 = 50$ km s^{-1} Mpc^{-1}.

SOURCES.—(1) Measured with Reticon spectrograph of du Pont 2.5 m telescope; (2) this paper; (3) Zwicky 1971; (4) visual estimate from POSS or SRC(J) to nearest 0.5 mag; (5) de Vaucouleurs, de Vaucouleurs, and Corwin 1976; (6) Zwicky, Herzog, and Wild 1961.

objects as defined above. No galaxy imaged so far with a large telescope matches Hoag's object in circular symmetry, probably because few are as symmetrical to start with and partially also because few are seen as nearly face-on.

d) Accretion Hypothesis

What mechanism could lead to the formation of Hoag-type galaxies? We have pointed out above that the bar instability envisaged by Brosch (1985) needs a central disk to operate, whereas the observed core of Hoag's object is a pure spheroid, and that the predicted lack of a massive halo in this galaxy is not confirmed by the measured high M/L ratio.

As an alternative hypothesis we propose that the formation of Hoag's object involved a major accretion event. There is mounting evidence that collisions between galaxies leading to mass transfers or even mergers play a major role in galaxy formation and evolution (for a review see Schweizer 1986). Specifically, it has been suggested that the formation of polar rings around S0 galaxies seems to be due to such mass transfers and mergers (Toomre 1977; Schweizer, Whitmore, and Rubin 1983). The recent discovery of faint ripples ("shells") around some specimens provides supporting evidence for this hypothesis (Schechter and Kristian 1984; van Gorkom, Schechter, and Kristian 1987; Whitmore, McElroy, and Schweizer 1987). Since accretion occurs presumably at random angles, one expects the formation not only of polar rings but also of transient inclined rings and of relatively stable equatorial rings. The low surface brightness and low star formation rate of the ring of Hoag's object seem to agree roughly with the corresponding quantities observed in polar-ring galaxies. Also, the fraction of all galaxies that are Hoag-type, $\sim 1 \times 10^{-3}$, is roughly equal to the fraction of galaxies with polar rings, as one might expect if the various rings are all formed by the same process. In this emerging picture, then, galactic disks grow episodically by accretion, and rings may simply be fragmentary disks.

We wish to emphasize, however, that in Hoag's object we have not found any tidal tail or ripple signature brighter than $g_0 \approx 28$ mag arcsec^{-2}, hence our reasoning remains conjectural. This absence of signatures suggests that the presumed accretion event took place at least 2–3 Gyr ago. Note also that from the available data we do not know the relative orientations of the rotation axes of spheroid and ring. We have assumed implicitly that they are parallel, but we cannot exclude other geometries, including an orthogonal orientation. Such an orientation would make Hoag's object an E0 galaxy with a polar ring.

There is one imperfection in Hoag's object that may eventually yield a clue about the galaxy's dynamics and recent evolution. Curiously, the brightest knots in the ring are not distributed at random, but are themselves aligned in a narrower ring which appears off-center from the main ring: this "braid in the ring" osculates the inner boundary of the main ring in the east, yet extends to nearly the outer boundary in the west (Fig. 1). This type of eccentric structure can hardly be in equilibrium, and remains to be explained.

We thank Rogier Windhorst and David Koo for obtaining CCD frames for us, James Gunn and Paul Schechter for valuable information concerning the instrumentation, Richard Stover and Tod Lauer for distributing their excellent VISTA software, Robert O'Connell and Morton Roberts for communicating unpublished results, and Noah Brosch for informing us of his results in advance of publication. One of us (R. I. J.) gratefully acknowledges support from a SERC/NATO Fellowship, and two others (F. S. and W. K. F.) acknowledge partial support from the National Science Foundation through grant AST 83-18845.

REFERENCES

Bottinelli, L., Gouguenheim, L., Paturel, G., and de Vaucouleurs, G. 1983, *Astr. Ap.*, **118**, 4.
Brosch, N. 1985, *Astr. Ap.*, **153**, 199.
Burstein, D., and Heiles, C. 1982, *A.J.*, **87**, 1165.
Buta, R. 1986, *Ap. J. Suppl.*, **61**, 609.
Carter, D. 1978, *M.N.R.A.S.*, **182**, 797.
de Vaucouleurs, G. 1953, *M.N.R.A.S.*, **113**, 134.
de Vaucouleurs, G., de Vaucouleurs, A., and Corwin, H. G. 1976, *Second Reference Catalogue of Bright Galaxies* (Austin: University of Texas Press).
Freeman, K. C. 1970, *Ap. J.*, **160**, 811.
Gunn, J. E., *et al.* 1984, *Bull. AAS*, **16**, 477.
Haynes, M. P., and Giovanelli, R. 1984, *A.J.*, **89**, 758.
Hoag, A. A. 1950, *A.J.*, **55**, 170.
Hubble, E. 1930, *Ap. J.*, **71**, 231.
Kennicut, R. C., and Kent, S. M. 1983, *A.J.*, **88**, 1094.
Kent, S. M. 1983, *Ap. J.*, **266**, 562.
Kormendy, J. 1977, *Ap. J.*, **218**, 333.
———. 1980, in *ESO Workshop on Two Dimensional Photometry*, ed. P. Crane and K. Kjär (Geneva: ESO), p. 191.
———. 1985, *Ap. J.*, **295**, 73.
Kormendy, J., and Illingworth, G. 1982, *Ap. J.*, **256**, 460.
Lauer, T. R. 1985, *Ap. J. Suppl.*, **57**, 473.
Lauer, T. R., Stover, R. J., and Terndrup, D. 1983, *The VISTA User's Guide* (Lick Obs. Tech. Rept. 34) (Santa Cruz: University of California at Santa Cruz).
Lynds, R., and Toomre, A. 1976, *Ap. J.*, **209**, 382.
O'Connell, R. W., Scargle, J. D., and Sargent, W. L. W. 1974, *Ap. J.*, **191**, 61.
Oke, J. B., and Gunn, J. E. 1982, *Pub. A.S.P.*, **94**, 586.
Pence, W. 1976, *Ap. J.*, **203**, 39.
Rainey, G. W. 1977, Ph.D. thesis, University of California, Los Angeles.
Reynolds, J. H. 1913, *M.N.R.A.S.*, **74**, 132.
Rubin, V. C., Burstein, D., Ford, W. K., Jr., and Thonnard, N. 1985, *Ap. J.*, **289**, 81.
Sandage, A. 1961, *The Hubble Atlas of Galaxies* (Washington, DC: Carnegie Institution of Washington).
Sargent, W. L. W., Schechter, P. L., Boksenberg, A., and Shortridge, K. 1977, *Ap. J.*, **212**, 236.
Schechter, P. L., and Kristian, J. 1984, *Carnegie Inst. Washington Yearbook*, **83**, 50.
Schweizer, F. 1981, *A.J.*, **86**, 662.
———. 1986, *Science*, **231**, 227.
Schweizer, F., Whitmore, B. C., and Rubin, V. C. 1983, *A.J.*, **88**, 909.
Simkin, S. M. 1974, *Astr. Ap.*, **31**, 129.
Theys, J. C., and Spiegel, E. A. 1977, *Ap. J.*, **212**, 616.
Thonnard, N., Rubin, V. C., Ford, W. K., Jr., and Roberts, M. S. 1980, *Carnegie Inst. Washington Yearbook*, **79**, 573.
Thuan, T. X., and Gunn, J. E. 1976, *Pub. A.S.P.*, **88**, 543.
Tonry, J. L. 1984, *Ap. J.*, **279**, 13.
Toomre, A. 1977, in *Evolution of Galaxies and Stellar Populations*, ed. R. B. Larson and B. M. Tinsley (New Haven: Yale University Observatory), p. 401.
van Gorkom, J. H., Schechter, P. L., and Kristian, J. 1987, *Ap. J.*, **314**, 457.
Vorontsov-Vel'yaminov, B. A. 1960, *Soviet Astr.—A.J.*, **4**, 365.
Wade, R. A., Hoessel, J. G., Elias, J. H., and Huchra, J. P. 1979, *Pub. A.S.P.*, **91**, 35.
Whitmore, B. C., and Kirshner, R. P. 1981, *Ap. J.*, **250**, 43.
Whitmore, B. C., McElroy, D. B., and Schweizer, F. 1987, *Ap. J.*, **314**, 439.
Zwicky, F. 1971, *Catalogue of Selected Compact Galaxies and Post-eruptive Galaxies* (Guemligen: F. Zwicky), p. 249.
Zwicky, F., Herzog, E., and Wild, P. 1961, *Catalogue of Galaxies and of Clusters of Galaxies* (Pasadena: California Institute of Technology), Vol. **1**.

W. KENT FORD, JR., and FRANÇOIS SCHWEIZER: Department of Terrestrial Magnetism, Carnegie Institution of Washington, 5241 Broad Branch Road, N.W., Washington, DC 20015
RICCARDO GIOVANELLI: Arecibo Observatory, P.O. Box 995, Arecibo, PR 00613
ROBERT JEDRZEJEWSKI: Mount Wilson and Las Campanas Observatories, 813 Santa Barbara Street, Pasadena, CA 91101

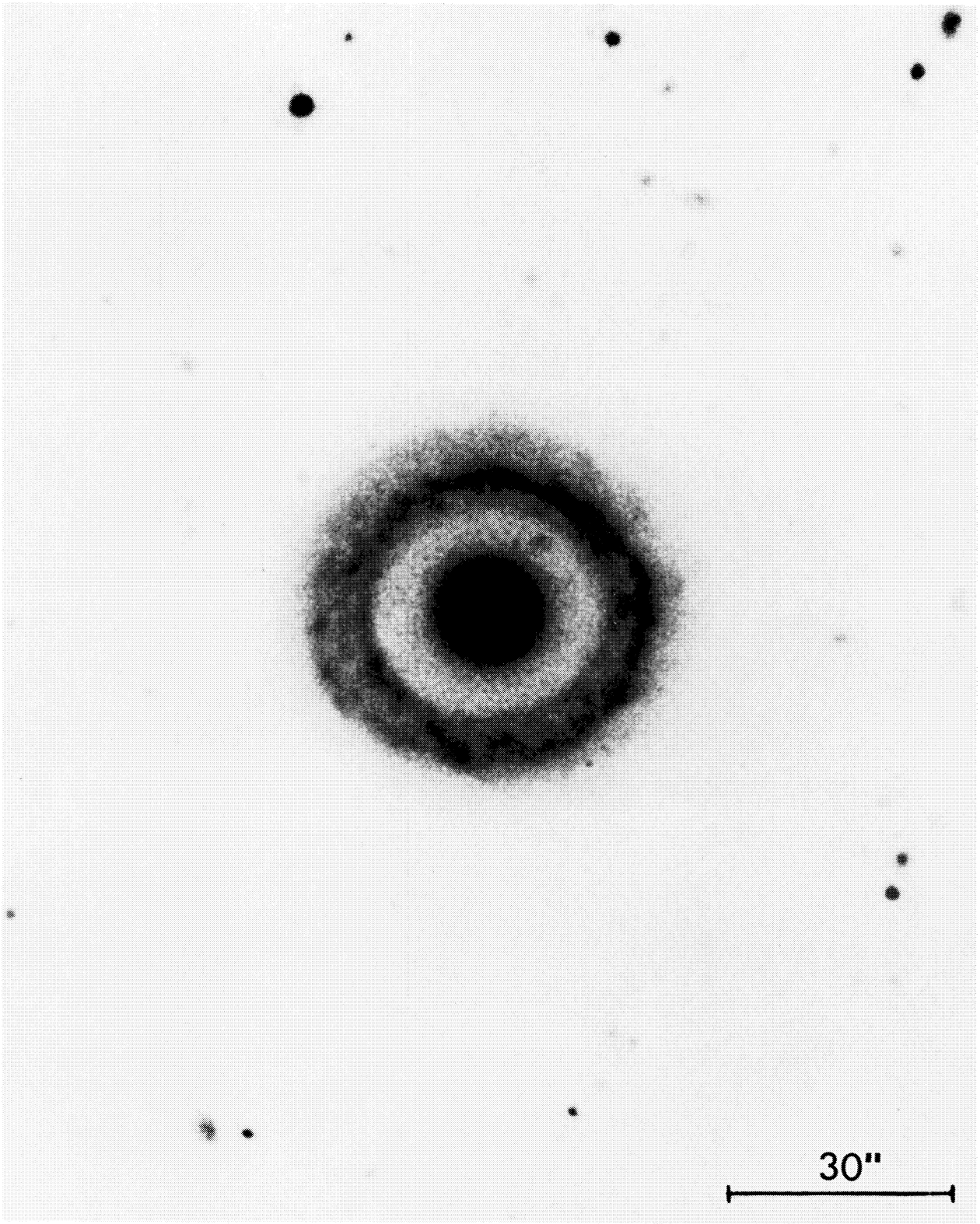

FIG. 1.—Broad-band image of Hoag's object showing the central core and surrounding ring; reproduced from two summed *g* frames obtained with the Hale 5 m telescope and 4-Shooter camera in 1.″05 seeing (FWHM). The total integration time was 10 minutes. The field shown measures 390 × 490 pixels = 2.′2 × 2.′7; north is up, and east is to the left. Note the apparent gap between core and ring and the knotty structure of the ring.

PLATE 12

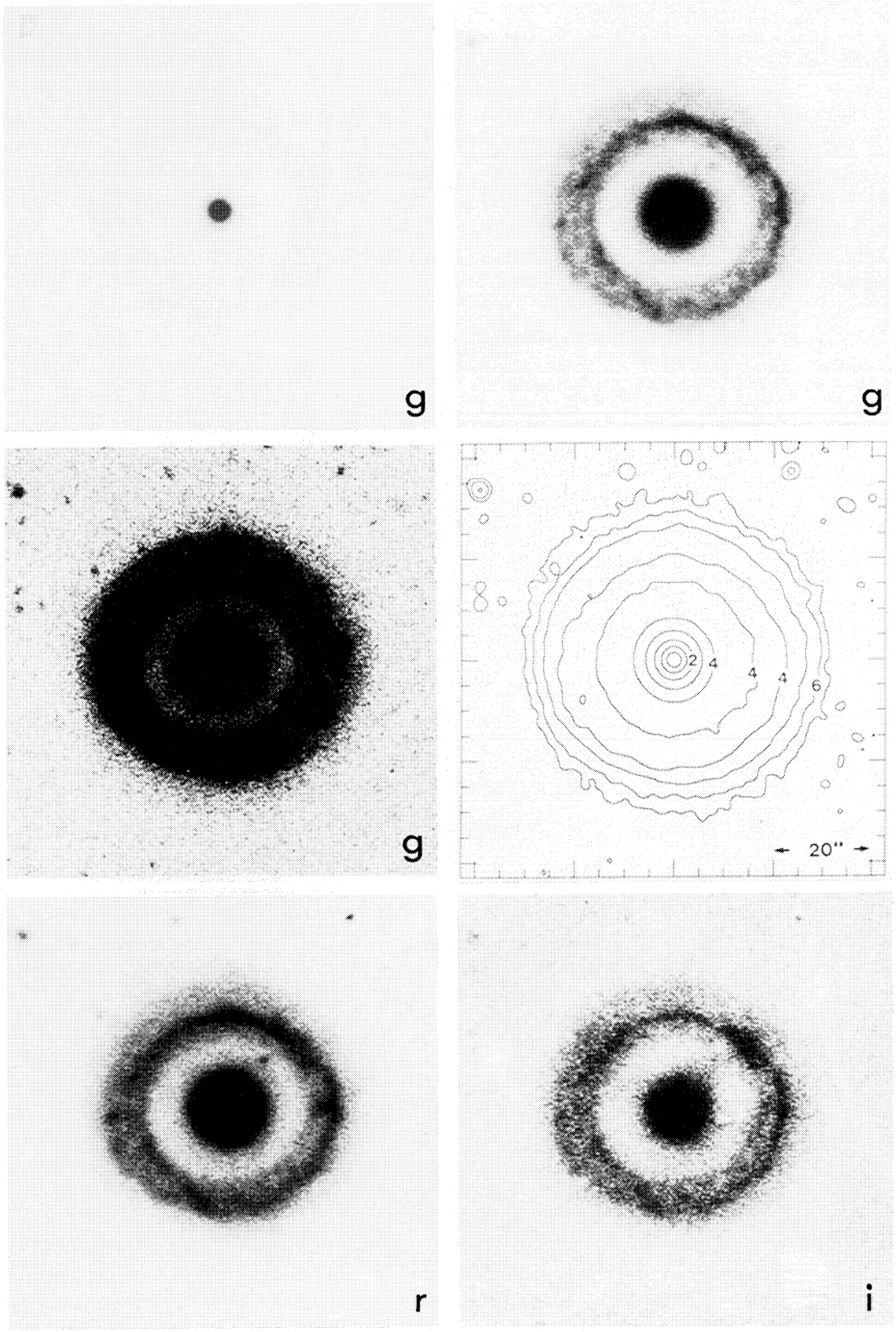

FIG. 2.—Hoag's object imaged in the g, r, and i passbands with the Hale 5 m telescope and 4-Shooter camera. The top four panels show a central 1'.4 × 1'.4 portion of the same image as Fig. 1, displayed at three different contrasts and as a smoothed isophotal map (with isophotes spaced 1 mag apart and labeled 2, 4, and 6 at $g_0 = 22$, 24, and 26 mag arcsec^{-2}, respectively). The two bottom panels show an r image, exposed for 5 minutes through slight cirrus, and an i image, exposed for 6 minutes through heavy cirrus; some defects have been interpolated across. Note how the "gap" between core and ring fills in at high contrast, and the similar appearance of the ring in the g, r, and i images.

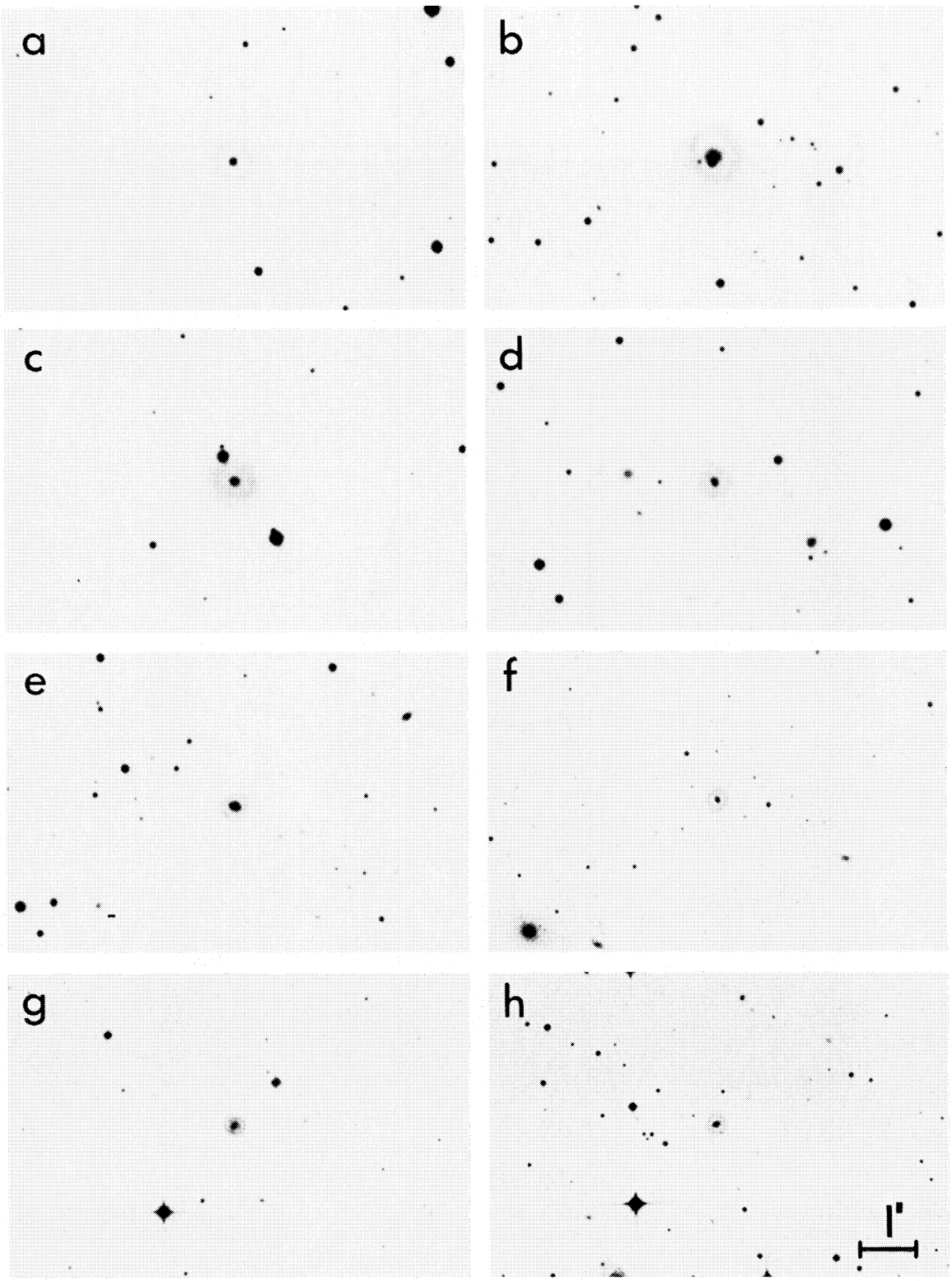

FIG. 7.—Eight Hoag-type galaxies, reproduced at a uniform scale. North is up, and east is to the left. (*a*) Hoag's object; (*b*) NGC 6028; (*c*) MCG−2-33-25; (*d*) A1519.6+5451; (*e*) Zw 167.025; (*f*) A0036.4−3905; (*g*) A0247.9−4015; and (*h*) A0452.3−4256. Data on these galaxies are summarized in Table 4. (Panels *a–e* are reproduced from the blue prints of the Palomar Observatory Sky Survey, and panels *f–h* from the J films of the ESO/SRC Sky Survey.)